Luminosity Measurements from Virtual Compton Scattering

D. Roff
H.H. Wills Physics Laboratory, University of Bristol, UK.

Abstract

Virtual Compton scattering can be used as a way of monitoring the luminosity at HERA. Using Compton events a result of $2.957 \pm 0.091(\mathrm{stat})\ {}^{+0.142(\mathrm{syst})}_{-0.078(\mathrm{syst})}\ \mathrm{pb}^{-1}$ was obtained for the luminosity of the 1994 data. This is within statistical and systematic error of the value given by the existing luminosity monitor which is given as $2.988 \pm 1.5\%\ \mathrm{pb}^{-1}$.

1 Introduction

The leading contributions to radiative elastic and inelastic positron-proton scattering are shown in the diagrams of Fig. 1.

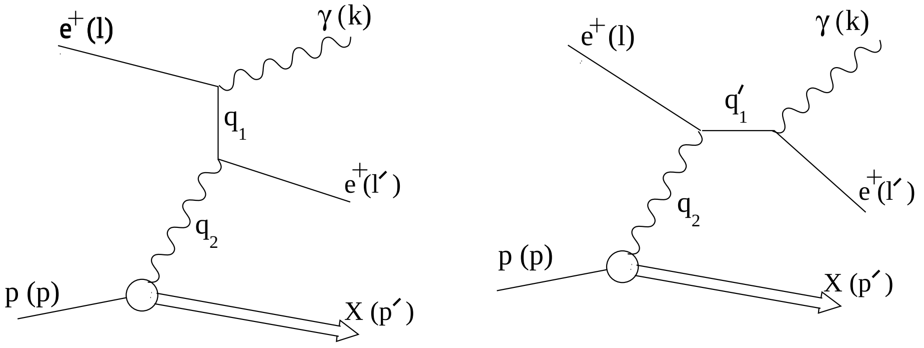

Figure 1: The Feynman diagrams for the process $e^+p \to e^+\gamma X$.

The four-vectors of the ingoing and outgoing particles are denoted by p (incident proton), l (incident positron) , p' (hadronic final state, in the elastic case this is the proton), l' (scattered positron) and k (radiated photon). The radiative scattering cross section is largest near the poles of the virtual electron and the virtual photon propagators. Three classes of radiative processes can be distinguished [1]:

1. The **bremsstrahlung process** which is characterized by $q_2^2 \to 0$ and $q_1^2, q_1'^2 \to 0$ where both scattered positron and photon travel in the direction of the incident electron beam. In this case the cross section is very large and this reaction is used in the standard method of luminosity determination for the HERA collider experiments.
2. The **QED Compton process** where $q_2^2 \to 0$ but q_1^2 and $q_1'^2$ are finite. This class of events can be regarded as scattering of a quasireal photon off an positron leading to finite scattering angles of both positron and photon which thus can be measured in the main detector. This process and the bremsstrahlung process can be represented by identical Feynman diagrams but occur in different kinematic regions. It this process that will considered in this note.
3. The **radiative DIS process** which is characterized by a large absolute value of q_2^2 and $q_1^2, q_1'^2 \to 0$. In this class of events the radiated photon moves along the direction of the incident or the scattered positron and in the latter case cannot be resolved from the positron.

The QED Compton process which we deal with in the following is thus characterized by a large mass of the virtual positron. Since the four-momentum transfer between the proton and the positron is very small, the positron-photon system and the hadronic final state both have transverse momenta close to zero. The hadronic final state thus leaves the detector through the beam hole in most of the cases.

The dominant contribution to QED Compton scattering is the elastic reaction $e^+p \to e^+\gamma p$ [2]. Since the elastic form factors of the proton are well known the cross section of the elastic channel can be precisely calculated. There are additional inelastic contributions to the QED Compton process, but these are small if the four-momentum transfer, $Q^2 = -q^2$, is small.

In the next section details of the present luminosity monitor are given together with its limitations after the planned HERA upgrade. As the current method of luminosity measurements, using a photon calorimeter for Bremsstrahlung reconstruction, will be difficult or even impossible to apply after the HERA upgrade, the potential of the QED Compton process as an alternative luminosity measurement is being investigated. The signature of the Compton peak is then defined as well as some useful quantities used in the analysis. Then details of the cuts imposed on the data are given. Section 4 includes a description of the Monte Carlo simulation of the Compton events. Finally the result and its associated errors of the luminosity calculated from the Compton events are derived and compared to that value given by the LUMI.

2 The Luminosity Monitor (LUMI)

Measurement of the bremstrahlung process, $e^+p \rightarrow e^+\gamma p$, used for the luminosity monitoring is based on the detection of a final state photon which is emitted at very small angles with respect to the initial positron direction. The luminosity monitor consists of the photon detector close to the proton beam pipe at a distance of -107m and an positron detector near the positron beam at a distance of -35m. A detailed description of the luminosity monitor is given in [3].

However, the planned increase in HERA luminosity and the associated ZEUS upgrades will mean that some components will exceed their technical limits. The LUMI is one of these components. With the planned increase in bending radius of the positron beam, the thickness of the carbon filter in front of the photon calorimeter of the luminosity monitor would have to be increased from 2-3 radiation lengths (X_0) to 4 X_0. This would degrade the resolution from the present $23\%/\sqrt{E}$ (for 2 X_0) to greater than $50\%/\sqrt{E}$, and increase the minimum energy that can be well measured from 1 GeV to about 5 GeV. The expected degradation of the luminosity measurement due to this effect is greater than 2% which is not compatible with the required precision of 1%.

The strongly increased event rate will also cause considerable problems. Firstly, at a luminosity of $10^{32}/\mathrm{cm}^2\mathrm{s}$ the rate of bremstrahlung with energy above 1 GeV is 17 MHz [4]. This results in a very high occupancy. Effects of such event pileup would have to be controlled by usage of different energy cuts. Secondly, the luminosity detector is readout by PMTs. If one scales the present anode current (already at very low HV) to a luminosity of $10^{32}/\mathrm{cm}^2\mathrm{s}$ one expects $60\mu\mathrm{A}$. Either low gain or hybrid PMTs would then have to be used. Finally, the radiation dosage at the worst point is expected to be up to 100kGray/year, which is possibly fatal for the scintillator calorimeters. In addition the photon acceptance will be reduced from 98% to 80%. Hence systematic effects are much less controlled and may result in an error from this source which increases from 0.5% to 2% at the full luminosity [4].

Therefore, a luminosity measurement similar to the one presently used will have an estimated accuracy of 5%. To achieve approximately 1%, desired for physics analysis, alternative solutions have to be found. One such solution could be to make use of virtual Compton scattering to monitor the luminosity.

3 The Compton Peak

In the calculation of radiative corrections to neutral current deep inelastic scattering in the leading logarithmic approximation [5], one may decompose the total cross section into parts associated not only with initial and final state radiation, but also a part associated with the nearly collinear emission of the exchanged photon from quarks or from the proton, the so called Compton peak. Since this cross section can be calculated precisely in QED, and is relatively large one can use a Compton event sample for an indepedent cross check of the measurement of the integrated luminosity delivered by HERA.

The experimental signature of Compton peak events is an positron-photon pair, which are emitted at small angles with respect to the positron beam direction and which have $l'_t \approx k_t$, where l'_t and k_t is the tranverse momentum of the scattered positron and photon respectively. For the majority of the Compton events there is little or no hadronic activity, the nucleon continuing along the beam pipe. Nearly all of these events are thus detected in the rear part of the calorimeter (RCAL), and almost no events are found in the barrel (BCAL) or forward (FCAL) parts of the calorimeter. Most of the detected events are found within the acceptance of the small angle rear tracking detector (SRTD) [7] which covers polar angles in the interval $162° < \theta < 176°$. The most important detector components in this analysis are therefore the RCAL and the SRTD. Since the average scattering angle of the positrons is small, only a small fraction of the events have an associated track in the central tracking detector (CTD) and therefore only these events have a reconstructed vertex.

4 Monte Carlo

The elastic Compton Monte Carlo (MC) events were generated using the Compton 2.00 program which is explained in more detail in [1]. The generated "Compton" events are defined as those experimental events in which one positron and one photon, almost coplanar, are observed at finite angles in the detector.

The elastic Compton events were generated within the ranges given in Table 1 for several kinematic variables. The COMPTON 2.00 program generates both elastic and inelastic Compton events. In the kinematic range considered 28% of the total cross section is due to inelastic Compton events and 72% due to elastic events. Note that even though the hadronic mass is generated, a detailed description of the final hadronic components is not given. A total of 32179 elastic Compton events were generated with a corresponding cross section of $2263.4 \pm 1.3\,(stat)$pb. Also 2194 inelastic Compton events were generated with a cross section of $710 \pm 0.9\,(stat)$pb.

Parameter		Range	
		Minimum	Maximum
Acollinearity	[degree]	0	45
Positron Energy ($\mathrm{E_e}$)	[GeV]	27.5	
Proton Energy ($\mathrm{E_p}$)	[GeV]	820.0	
θ_e, θ_γ	[degree]	3	177
$\mathrm{p_T}$	[GeV/c]	0	20
Positron Energy ($\mathrm{E'_E}$)	[GeV]	5.0	-
Photon Energy ($\mathrm{E_\gamma}$)	[GeV]	5.0	-
Energy Sum ($\mathrm{E'_e + E_\gamma}$)	[GeV]	10.0	-
Invariant Mass ($\mathrm{M_{e\gamma}}$)	[GeV/c^2]	1.0	300

Table 1: The range of kinematic variables used with the COMPTON 2.00 program.

DIS events were generated using HERACLES + ARIADNE, with $Q^2 > 3.3$ GeV^2, which acted as a check on the background. The hadronic final state was simulated using the colour-dipole model as implemented in ARIADNE [8] for the QCD cascade and JETSET [9] for the final hadronisation. In

HERACLES [10] the radiative cross section is divided into three channels. These channels correspond to the three peaks in the leading logarithm approximation to the full $\mathcal{O}(\alpha)$ calculation: ie initial and final state radiation and Compton radiation. It was found that the only DIS events to survive the cuts were the inelastic Comptons generated by HERACLES and scaled accordingly, no events contributed to the final sample.

5 Event Selection

An initial sample is selected for analysis by requiring that the events pass at least one of the following first level triggers. We require that an "isolated" positron is found in the rear calorimeter (RCAL), or that the total energy deposited in the RCAL is above the threshold value of 3.4 GeV, or that the total energy deposited in the barrel calorimeter (BCAL) is above the threshold value of 4.78 GeV. At the pre-selection stage we require that the electron finder locates two or more "electron" candidates of energy greater than 1 GeV and probability greater than 0.5. After this initial selection $\sim 1.7 \times 10^6$ events remained from the 1994 data.

The selected data was then subjected to stricter cuts which are listed below.

- Only two "electron" candidates (electromagnetic energy deposits) with neural net electron finder (SINISTRA 95), both with probabilities greater than 0.9, are found.
- The energy of both candidates as measured by the calorimeter or SRTD must be greater than 8.0 GeV.
- To remove the final state radiation background we require that $\mid \pi - \Delta\phi \mid < 10°$. This quantity is known as the acollinearity and is a measure of the tranverse momentum balance of the out going particles, where $\Delta\phi$ is the difference between the azimuthal angle of the positron and the photon.
- To remove the DIS background we require that $\mid \theta_e - \theta_\gamma \mid < 85°$, where θ_e and θ_γ are the polar angles of the positron and the photon respectively.
- The total energy measured by the calorimeter minus that of the positron-photon pair, ie the hadronic component, < 2 GeV. This reduces the contamination by inelastic Compton events.
- A box cut of 13cm $\times$ 13cm around the beam pipe and ensures that the energy deposited is fully contained within the calorimeter. The particles must be produced at large angles otherwise they will be lost down the beam pipe. This not only eliminates a large number of events, but suppresses most significantly initial state radiation events relative to final state and Compton events.
- A requirement that no more than one cluster has an associated track is imposed and that this track originates from the interaction point.
- The total $E - p_z$ of the event must be in the range $20\,\mathrm{GeV} - 65\,\mathrm{GeV}$.

Further to the above cuts it is required that the SRTD hits are unambiguous; that is, that the strip with the highest energy does not occur on the edge or on a crack of the STRD. After the above cuts 1289 Compton candidates, 5818 elastic MC candidates, and 187 inelastic MC candidates remained. The DIS contribution estimated from MC was negligible.

6 Results and Conclusions

6.1 Calculations

The results of these cuts on Data and Monte Carlo is shown in the four distributions of Fig. 2.

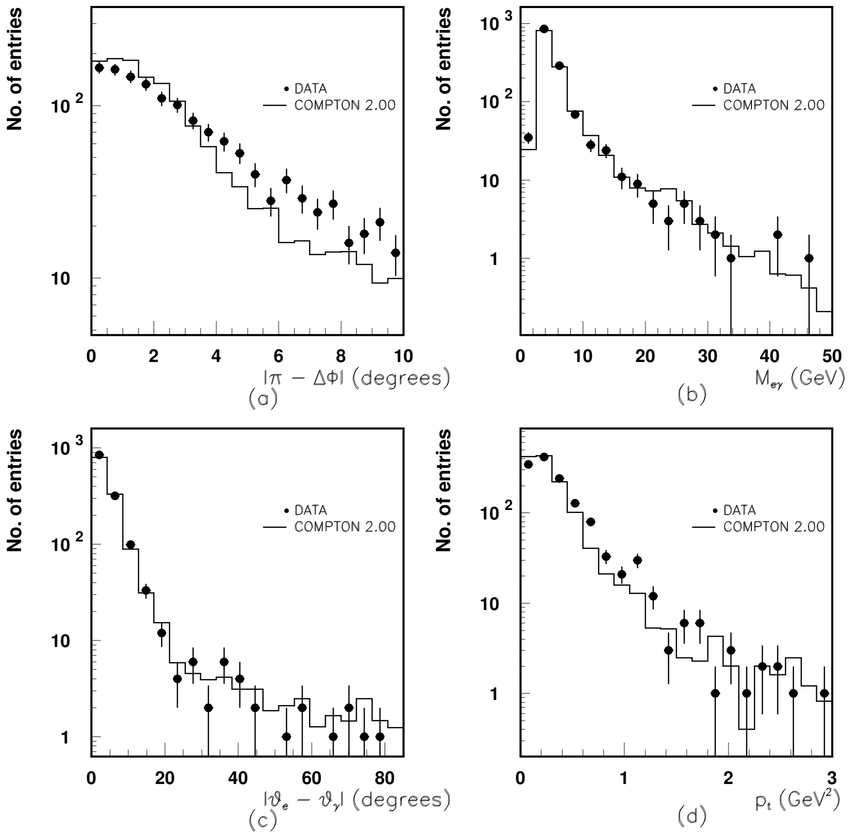

Figure 2: Graphs showing: (a) The distribution of the acollinearity, $|\pi - \Delta\phi|$, (b) the distribution of the square of the invariant mass of the positron-photon system, (c) The distribution of the quantity $|\theta_e - \theta_\gamma|$, and (d) The $\mathrm{p_t}$ distribution for the Compton candidates. The data points are represented by symbols and MC by histograms. For all plots, the elastic MC is normalised to the data luminosity and contains an inelastic contribution of 6% (see section 6.2).

As expected the distributions for the modulus of the acollinearity ($|\pi - \Delta\phi|$) and the transverse momentum ($\mathrm{p_t}$) peak at zero. These are shown in Fig. 2a and Fig. 2d respectively. In Fig. 2a the discrepancy between data and MC is believed to be due the presence of additional dead material. The lower energy components of the subsequent showers are therefore more affected by the magnetic field. Hence the path of the positrons is bent slightly so that the positron and photon are no longer back-to-back. Fig. 2b shows the distribution of the invariant mass of the positron-photon system, $M_{e\gamma}$. The existence of an excited electron state would become evident via a peak in the distribution of the invariant mass. Up to 50 GeV no such peak was found. The polar angle difference of the positron-photon pair in shown in Fig. 2c and peaks at zero.

The integrated luminostiy was calculated using the equation,

$$\int \mathcal{L} = \frac{\mathrm{N}}{\sigma \mathrm{A}}. \tag{1}$$

$$\begin{aligned} \mathrm{N} &= \text{The corrected number of elastic Compton candidates} \\ &= 1210 \pm 34.78\,(stat)\ \text{candidates} \end{aligned}$$

$$\begin{aligned} \mathrm{A} &= \text{Acceptance} \\ &= \frac{\text{Number of MC candidates after cuts}}{\text{Number of MC candidates generated}} \\ &= \frac{5818}{32179} \\ &= 0.181 \pm 0.001\,(stat) \end{aligned}$$

$$\begin{aligned} \sigma &= \text{cross section for the MC generated Comptons} \\ &= 2263.4 \pm 1.3\,(stat)\ \text{pb} \end{aligned}$$

This gives a value of,

$$\int \mathcal{L} = 2.957 \pm 0.089\,(stat)\ \text{pb}^{-1} \tag{2}$$

or,

$$\int \mathcal{L} = 2.957 \pm 3.01\%\,(stat).$$

6.2 Calculating the Inelastic Compton Contribution

Within the data sample of elastic Compton candidates there is a small contamination of inelastic Comptons. These are misidentified as the proton remnants disappear undetected down the beam pipe. To allow for this contamination an amount of inelastic MC is then added to the elastic MC. The optimun level of contamination was calculated using a χ^2 fit of the data and MC distributions for the four plots shown in Fig. 2. Where as the elastic MC was scaled to the data luminosity the scale for inelastic MC was varied to obtain a minimum χ^2 value. The results of these fits are shown in Fig. 3.

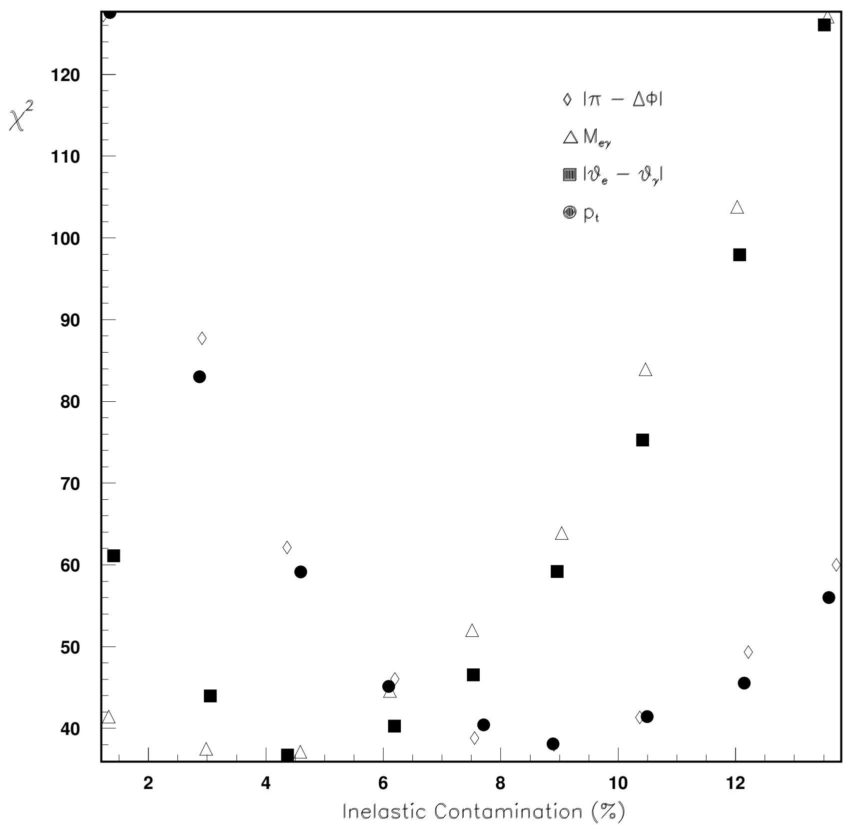

Figure 3: Graph showing χ^2 value versus scale value for the inelastic Compton contribution.

The average of the minima of the four curves was taken resulting in an inelastic Compton contribution of $\sim 6\%$ to be added to the elastic Compton sample.

6.3 Systematic Errors

The systematic errors were estimated by varying the applied cuts by plus/minus one standard deviation around their nominal value. The resolution of each variable cut on was measured using the Monte Carlo (ie $X_{\mathrm{meas}} - X_{\mathrm{true}}$). The results are shown below in Table 2.

Variable	Adjustment	% Change to $\int \mathcal{L}$
boxcut (13cm)	14cm	+0.74
delta-phi cut ($\lvert\pi - \Delta\phi\rvert < 10°$)	$< 7.755°$ $< 12.245°$	-1.39 +2.40
energy cut (8 GeV)	7 Gev 9 GeV	-1.22 +0.00
theta-diff cut ($\lvert\theta_e - \theta_\gamma\rvert < 85°$)	$< 84°$ $< 86°$	-0.03 +0.00
probcut ($\mathcal{P}_e, \mathcal{P}_\gamma > 0.9$)	e-finding efficiency $\pm 10\%$	-1.15 +1.18
z-vertex cut ($\mathrm{z - vertex} < \lvert 50\mathrm{cm}\rvert$)	-40cm-30cm $\pm$90cm	-1.45 +3.59
track cut (no. of tracks < 2)	< 3	+1.59
$\mathrm{E - p_z}$ cut (20-65 GeV)	30-65 GeV 20-75 GeV	-0.24 +0.00
% inelastic Comptons (6%)	3% 9%	+2.07 -2.9

Table 2: Table showing the systematic errors of the luminosity measurement after adjusting the applied cuts. Nominal values of the cuts are shown in brackets.

A better understanding or removal of the dead material in the detector would reduce the systematic error in the acollinearity measurement. Consideration was given to the difference between the electron finding efficiencies of SINISTRA 95 for data and MC. An improvement could be achieved by studying the 'electron' finding efficiency of SINISTRA 95 in different regions of the calorimeter. The systematic errors could be reduced further by better calibration for low energy positrons/photons. The systematic errors due to the inelastic Compton contamination could be greatly reduced if the MC described the final hadronic components and one would expect to see the level of contamination to decrease.

Even though most of the systematic uncertainties can be reduced by an improved understanding of the detector and the applied algorithms, the contribution from the satellite bunches is the source of the large systematic error the z-vertex cut. As this effect does not depend on the ZEUS detector but on the beam conditions this is difficult to understand and simulate completely. Unless a significantly better comprehension of the proton satellite bunches is gained, the uncertainty from the vertex distribution can only be reduced if HERA manages to avoid them completely. The possibility that this situation will occur will only become evident after the HERA upgrade.

So the resultant value for the luminosity is,

$$\int \mathcal{L} = 2.957 \pm 0.091(\mathrm{stat})\,^{+0.142(\mathrm{syst})}_{-0.078(\mathrm{syst})}\ \mathrm{pb}^{-1} \tag{3}$$

or,

$$\int \mathcal{L} = 2.957 \pm 3.1\%(\mathrm{stat})\,^{+4.8\%(\mathrm{syst})}_{-2.6\%(\mathrm{syst})}$$

7 Conclusion

An alternative method for calculating the luminosity at HERA is presented in this paper, the motivation being that the present luminosity monitor will be inadequate when HERA is upgraded. The integated luminosity value for the 1994 obtained by the LUMI is $2.988 \pm 1.5\%\ \mathrm{pb}^{-1}$. Comparing this value to the result $2.957 \pm 0.091(\mathrm{stat})\,^{+0.142(\mathrm{syst})}_{-0.078(\mathrm{syst})}\ \mathrm{pb}^{-1}$ $\left(2.957 \pm 3.1\%(\mathrm{stat})\,^{+4.8\%(\mathrm{syst})}_{-2.6\%(\mathrm{syst})}\right)$ obtained from the analysis of virtual Compton scattering events one can see that they are in good agreement and within experimental error. With improved knowledge of the detector and provided the beam filling in HERA can be controlled such that little or no satellite bunches occur then it will most likely be possible to use QED Compton scattering events to measure the integrated luminosity with an error of the order of 1%, for ZEUS in the future. It should be noted that the lack of statistics makes this method unfeasible for run-by-run calculations of the luminosity but may be used for calculating integrated luminosities for longer periods of data taking.

Acknowledgements

I would like to take this opportunity to thank Dave Bailey and Arnulf Quadt for their guidance, comments and patience. Many thanks to Rik Yoshida and Jon Labs who started me off on this project. I would also like to thank Frank Zetsche for the elastic Compton Monte Carlo.

References

[1] T.Carli, A.Courau, S.Kermiche, and P.Kessler. Quasi-real QED Compton Monte Carlo. *Physics at HERA*, Vol 3:1468, 1991.

[2] A.Ebel and F.Zetsche. Analysis of Elastic Compton Scattering Events using the 1994 ZEUS Data. *ZEUS Note*, 96-020, 1996.

[3] ZEUS Collaboration. “The ZEUS Detector”. *Status Report*, 1993.

[4] HERA-ZEUS Upgrade Group. “ZEUS Interaction Region Upgrade”. *ZEUS Note*, 96-086, 1996.

[5] J.Kripfganz, H.-J.Möhring, and H.Spiesberger. . *Z.Phys.*, C49:501, 1991.

[6] J.Blümlein, G.Levman, and H.Spiesberger. . *Z.Phys.*, C49:501, 1991.

[7] J.Ng and W.Verkerke. An overview of SRTD Analysis. *ZEUS Note*, 95-037, 1995.

[8] ARIADNE 4.06: L.Lönnblad, LU TP-89-10. *Comp. Phys. Commun.*, **71**:15, 1992.

[9] PYTHIA 5.7 AND JETSET 7.4: T.Sjöstrand CERN-TH 7112-93 (1994). T.Sjöstrand, LU-TP-95-20.

[10] HERACLES 4.4: A.Kwiatkowski, H.J.Höhring, and H.Spiesberger. *Comp. Phys. Commun.*, **69**:155, 1992.